Response to the reviewers

The following color scheme is used in response to the reviewers:

- In blue color the response to the comments raised by the reviewers
- Highlighted in yellow color the modifications added to the manuscript

Response to Referee #1

This work presents an experimental and numerical investigation into the stiffness knockdown of GFRP laminates with artificially manufactured embedded wrinkle defects. Overall, the paper is well written, easy to understand and contains valuable information. A few queries are as follows:

The authors appreciate the positive comments. We considered all the queries raised relevant to improve the quality of the manuscript. The points are addressed as follows in the manuscript:

1) It appears that the experimental/computational excercise on stiffness evaluation is carried out at a stage when no global failure mode (such as delamination) has been triggred from the wrinkle. If so, can the authors please mention this fact clearly? This is important, since if the load level triggers damage, more pronounced difference in stiffness will be seen between the 'flat section' and 'wrinkle section'.

Agree with that, here what was added to the manuscript

Prior to testing, the specimens were polished with sandpaper and treated with a lacquer Acryl spray to increase the bonding strength and attenuate the effect of rough side borders (Yang, et al. (2019)). A numerical buckling analysis was conducted to verify that the sample length within the grip section was bellow the buckling limit under compression for the target load. A strain rate of 0.01 $\%/s$ was used for three elapsed cycles. As a loading, a tension-compression test with load amplitudes of $\pm$ 16 KN was applied over an external controlled program, which feeds the machine with a triangular ramp loading. According to the ISO-527-1 and ASTM-D3039 standards, the stiffness should be taken over a strain range of 0.2% (Iso E. 527-1. (2012), ASTM AM. ASTM D3039. (2017)). The load level is chosen such that the deformation exceeds this range but still stay bellow load-levels where damage initiation could be introduced. The tensile-compression strain was measured at the four channels of the clip gauge extensometer.

2) The authors have mentioned that the simplified surrogate model eliminates minute geometric details of ply folds and resin pockets, while the high fidelity model captures all these details. It would be good to include images of meshed finite element models of surrogate vs high fidelity models side by side and also compare the total number of elements . Since , the results in Figure 9 indicate that the surrogate model predictions for both type of wrinkles are very close to high fidelity models, it would be interesting to know the simplified meshing pattern that still produces an accurate results. Also, can the authors compare the computational time saving while using the surrogate model vs the high fidelity model?

The images of the finite element models were included accordingly. The changes are included in the manuscript as shown below:

4.2 Finite Element Model

The numerical simulations are conducted in ABAQUS standard version 2021, meaning that an implicit linear Newton Raphson solver is used to predict the model response. Two 2D models are obtained with geometrical parameters from the image based
165 geometric model described in section 4.1: a surrogate model (SM) and high fidelity model (HFM) as shown in Figure 6.

The HFM embodies the geometric complexities of the characteristic defect. Thus, the HFM refers alone to high fidelity geometric features represented in the numerical model. Both models (SM and HFM) present approximate the same degrees of freedom, which result in a similar calculation time performed within few minutes on a 16 CPUs Linux cluster. 2D 8-node plane stress elements with biquadratic reduced integration (CPS8R) are used to discretize the specimen geometry. However, in the
170 HFM the resin regions are represented by 6-node modified plane stress elements with hourglass control (CPS6M) as triangular elements enable mesh refinement with acceptable resolution within the region. The SM contain the same elements used in the HFM excepting the modified plane stress elements for the resin region, which is not represented. The characteristic element

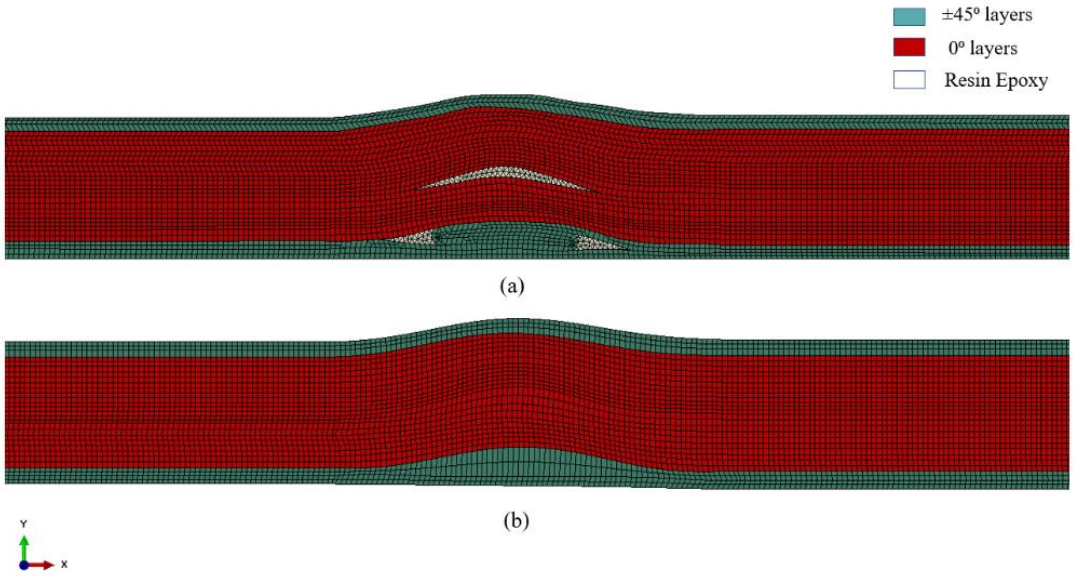

Figure 6. Comparison of mesh discretization with the geometric details of the wrinkle type 1 for the models: (a) HFM present the geometrical complexities of a fold wrinkle and resin pocket (b) SM present a simplified geometrical configuration.

3) Although shear loading in the wrinkle section and associated hysteretic loss in the resin is experimentally measured, the model does not assume any hysteretic damping effect. Can the authors suggest how their experimental finding on hysteresis loss be included in a future model development?

Indeed, at this point, the effect of the hysteresis loss is not accounted for in the model. The hysteresis loss experienced by GFRP is mainly related to the viscoelastic behaviour of the polymer matrix. The viscoelastic effect can be addressed by a material characterization including the viscoelastic properties in the model. Here is the modification in the text:

6 Results and Discussion

In this study, the stiffness is described as the overall slope of the stress versus strain relation. Thereby, stiffness values obtained from the experimental tests are measured of the slope load versus strain shown in Figure 9 and averaged by the mean cross-sectional area of the flat section for the two sets of specimens tested. As the wrinkle out of the straightness path results in a bending around the center of symmetry, strain results from the top and bottom of the wrinkle were averaged to account for the eccentricity effect. To preserve the correlation, the strain results from the top and bottom at the flat section were equally averaged. Figure 9 shows the hysteresis loop in detail for both types of wrinkle configurations and sections.

The hysteresis loss observed experimentally is mainly driven by the viscoelastic behaviour of the polymer matrix. Although not considered in the present numerical model, the viscoelastic effect can be addressed by using a visco-material law. The damping is calculated by averaging the hysteresis loop area over the three reversal cycles. The wrinkle section experience higher energy

Response to Referee #2

1) General: A good methodology and for the most part good and well-founded. The relatively small deviations also indicate a good simulation and the correct assumptions. The quality of the documentation can still be improved. The evaluation could be more precise. The material map is "strange" and the methods at the Matlab script call. Adapt the pictures accordingly.

The authors appreciate the positive feedback. We considered all the points raised which resulted in a significant improvement in the quality of the manuscript. The reply below refers to the comments that require a detailed explained response, whereas the minor corrections were modified straight in the text and highlighted in the pdf version submitted. The points are addressed as follows:

2) Please define the terms (wrinkles, fibre waviness, out-of-plane-wrinkling) more precisely. Wrinkles is equal to out-of-plane fibre waviness (see definition in Thor and Hallet 2020).

Thanks for this suggestion. This has been addressed in the following sentence:

1 Introduction

Wrinkles are manufacturing induced defects, which can impact the production cycle time leading to expensive repairs when required, ultimately resulting in a decline of wind turbine blades reliability. This study is dedicated to evaluate out-of-plane wrinkles due to its critical impact on the structural performance of the blade. Thus, the term wrinkles in this study are interpreted as out-of-plane wrinkles. Out-of-plane wrinkles is a result of fibre bending out of the laminate and layer bending through-thickness (Wang, L. (2001), Lightfoot, et al. (2013)). On the other hand, ply/fiber waviness is a fiber deviation from a straight alignment in a unidirectional laminate (Thor, et al. (2020)).

3) Are there also analytical models.

Below the modification in the manuscript:

Several methods are employed to represent wrinkles through numerical models (Leong, et al. a (2012), Leong, et al. b (2012),
40 Smith, et al. (2014), Mukhopadhyay, et al. (2015), Bender, et al. (2019), Xie, et al. (2018), Xie, et al. (2015)). Analytical models are equally described in the literature (Hsiao and Daniel a (1996), Hsiao and Daniel b (1996), Zhu, et al. (2015)). Finite element modelling is targeted in this work as it allows detailed representation of geometrical complex features. An idealized finite element model (FEM) based on the characteristic parameters of wrinkles was built with 3D solid elements (Leong, et al. a (2012), Leong, et al. b (2012)). Non-destructive test (NDT) imaging were converted into numerical models

4) If you want to keep the picture, please mark the place where it was taken in the cross-section on the left. Does it come from type 1 or 2 or from a place where both types look the same? Also scale indication of the plies-position to the respective position in the image.

The point was considered, here is the modification in the figure:

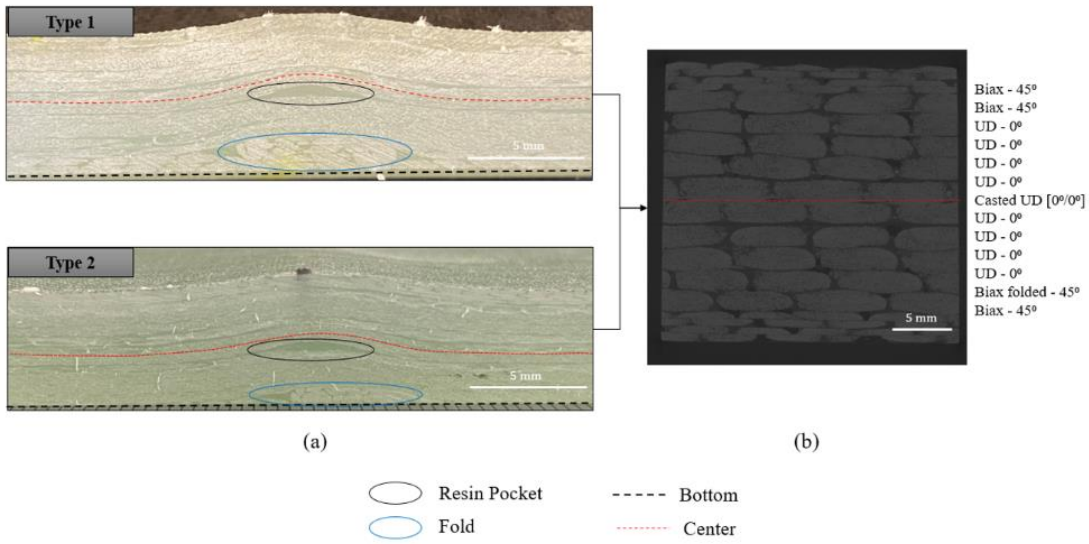

Figure 3. (a) Types of wrinkle configurations selected for the analysis; (b) Layup specification for the transverse cross section of the specimens taken at the flat region which is similar for both wrinkle types.

5) Table 2: for the UD layer, the same value is taken for all shear moduli, but the transverse contraction number is not. With BD, the shear modulus is varied and also the shear contraction coefficient. What material behaviour is assumed? Where do the characteristic values come from?

The 23 values have a neglected influence on the actual longitudinal stiffness of the model. The characteristic values were derived within the research project ReliaBlade.

Modifications in the manuscript follow below:

3.2 Manufacturing of Coupon Specimens

Coupon specimens are produced through two process phases with face sheets of glass fibre reinforced polymer (GFRP) consisting of uni-directional (UD), bi-directional (Biax) and resin epoxy. The UD ply thickness is 0.859 mm, whereas the Biax ply has 0.564 mm. Material properties are presented in Table 2. The transverse contraction values have a neglected influence on the actual longitudinal stiffness of the model. In principle E_{33} should be slightly lower than E_{22} due to the present of secondary oriented backing bundles in the x_2 direction, and accordingly the G_{13} compared to G_{12}. Nevertheless, those values are considered to have a negligible influence on the axial stiffness prediction which is dominated by the E_{11} and G_{12} components. In the first phase UD plies are laid on a mould to form a [0/0] panel. Two UD sheets are stacked together on top of an Aluminium cast mold with geometrical topology equivalent to the wrinkles type 1 and type 2 as defined in Table 1. The artificial defect is induced transversely to the orientation of the fibers along the panel width (Figure 4). Epoxy Hexion resin system with mixing

6) Method for filtering outliers very superficial. Name method of fitting technique (third step) - in the text it says polynomial was tested and in Figure 5 it says Fourier. Figure 5: Insert steps from text, numbers and font in diagram not recognizable. Where does the difference between the two models (surrogate & high fidelity) come from when the same steps are run through? How is the area described in the simplified model? - A picture would be desirable. Could this be made clear in the picture?

The authors combined the image processing toolbox available on Matlab with a series of encoded scripts to perform image processing, filtering, segmentation and fitting of each individual fiber. The filtering technique of the wrinkle image is based on rank filtering/median filtering, which removes outliers without reducing the resolution of the image. When it comes to the fitting technique, each individual fiber is evaluated accordingly to the least residuals which rule the best fit type adopted. Figure 5 was modified accordingly. The high fidelity model differs from the surrogate model in terms of geometrical features represented. That difference is explained in detail in section 4.2, where the difference between both models can be seen in Figure 6 of the updated manuscript version.

Modifications are done in the figures and in the manuscript accordingly:

4 Numerical Modelling

4.1 Image Based Geometric Model

Cross section images of the artificial defect are processed through Matlab-based scripted algorithms. The image processing scheme is performed in a five-step sequence (Figure 5) covering the steps of image processing, filtering, segmentation, fitting techniques for capturing the proper contour of an individual fiber and a 2D coordinate map generated to support the finite element modeling. A combination of the image processing toolbox available on Matlab with a series of encoded scripts are used for the image processing, filtering, segmentation and fitting of each individual fiber. The filtering technique of the wrinkle image is based on rank filtering /median filtering, which removes outliers without reducing the resolution of the image. When it comes to the fitting technique, each individual fiber is evaluated accordingly to the least residuals method.

For each defect configuration, two types of finite element models are derived: a surrogate model and a high fidelity model. The surrogate model solely accounts for the effect of individual ply waviness disregarding the effect of complexity geometry resultant from the fold in the Biax ply and resin regions. The high fidelity model regards the effects of resin regions and asymmetric wrinkle shapes resultant from the s-shaped Biax layer. The detailed finite element model is presented in Section 4.2.

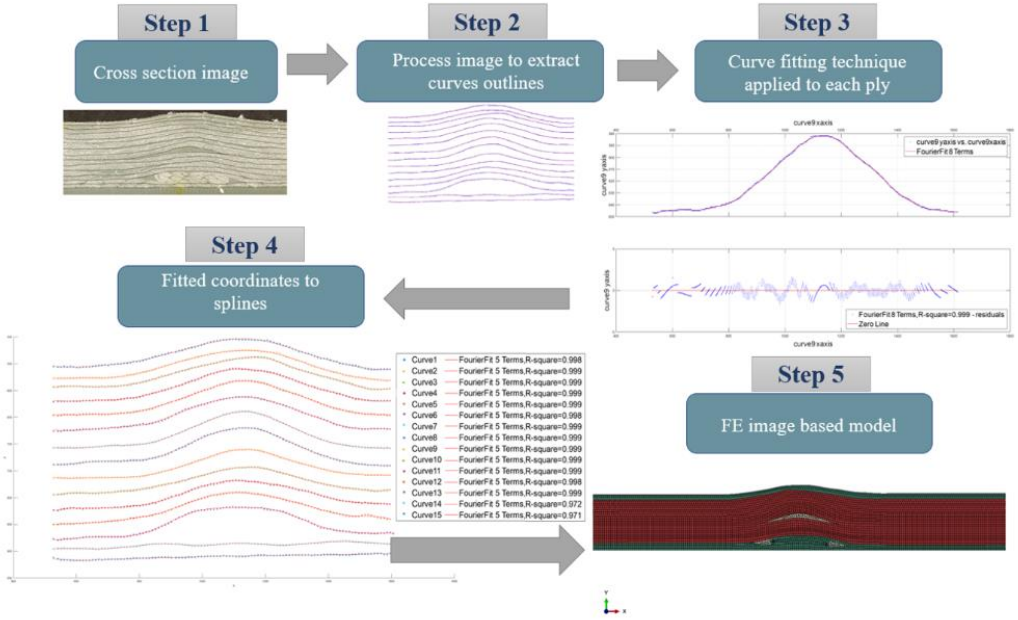

Figure 5. Four-step sequence to translate the cross section defect profile into a finite element model by thresholding individual contours, segmentation of such contours and outliers removal, mathematical fitting techniques to generate even spaced coordinates and finally the extraction of 2D coordinates to import into ABAQUS.

4.2 Finite Element Model

The numerical simulations are conducted in ABAQUS standard version 2021, meaning that an implicit linear Newton Raphson solver is used to predict the model response. Two 2D models are obtained with geometrical parameters from the image based geometric model described in section 4.1: a surrogate model (SM) and high fidelity model (HFM) as shown in Figure 6.

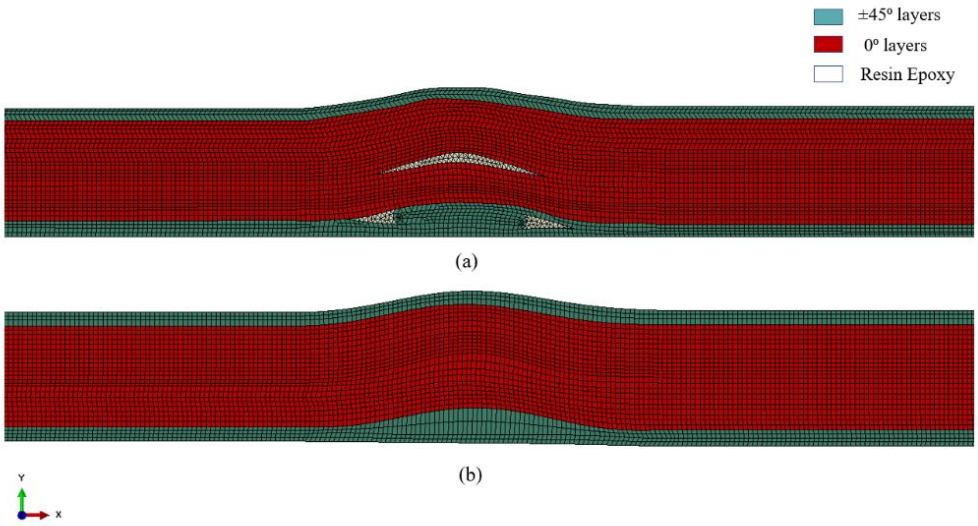

Figure 6. Comparison of mesh discretization with the geometric details of the wrinkle type 1 for the models: (a) HFM present the geometrical complexities of a fold wrinkle and resin pocket (b) SM present a simplified geometrical configuration.

7) Please state the measurement accuracy so that it is clear that you are not only recording measurement noise at a load of 16 kN. The results of the high-speed recordings are not discussed? Perhaps advertise here for another paper.

In this study, the samples were not driven to failure and the load was kept sufficiently slow to perform only stiffness measurements.

The manuscript was changed accordingly:

5 Experimental tests

Two specimens of each configuration type 1 and type 2 were tested under quasi-static loading with a servo-hydraulic tensile test machine Instron 8533, with load cell UK 084 and 250 ± 1.20 kN capacity. The specimens were mounted into grips with 50 mm gauge length extensometers, aligned back to back with the wrinkle in the center. For the flat section extensometers of

25 mm gauge length were positioned at a distance of 40 mm away from the wrinkle center. High-speed cameras were used to capture images of the side and back views of the gauge section as shown in Figure 8. The images from the camera are not relevant at this study as the samples are not driven to failure. In an upcoming study where the samples are tested under reverse fatigue the images are explored displaying the location for delamination initiation.

8) the yellow colour is difficult to see:

Change made accordingly below:

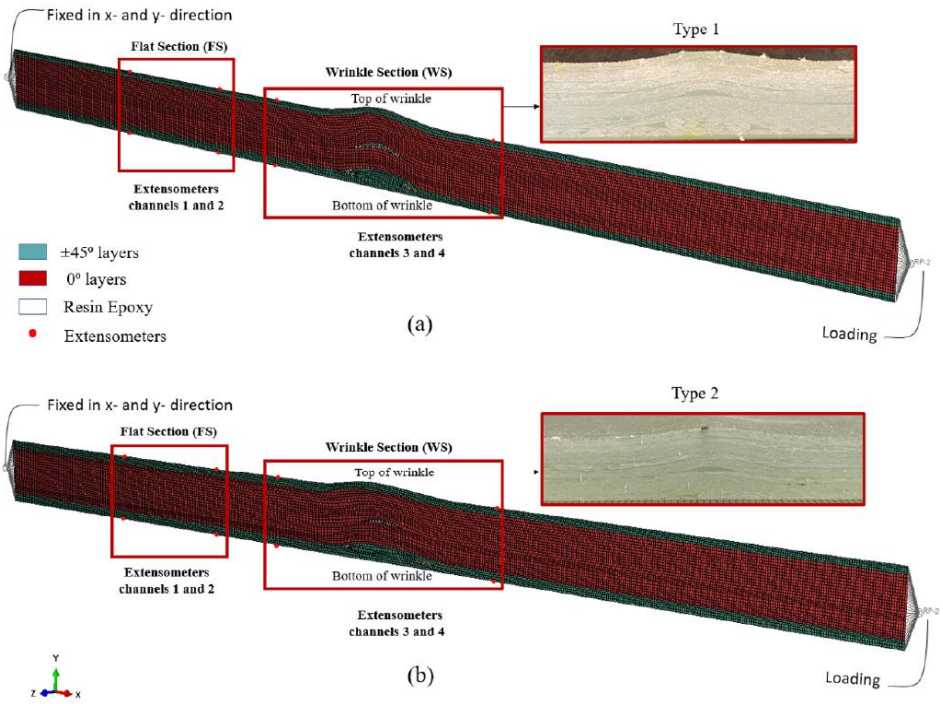

Figure 7. High fidelity finite element model modelled in a ply-by-ply sequence, with biaxial layers on top and bottom, UD layers in between and resin pocket around the biax fold and underneath the ply contour of max. amplitude : (a) coupon specimen model for wrinkle type 1 (b) coupon specimen model for wrinkle type 2.

9) Please, explain why the amplitude was chosen? Is a load-dependent increase in material damage to be expected at 16 kN?

Modification done as follows:

Prior to testing, the specimens were polished with sandpaper and treated with a lacquer Acryl spray to increase the bonding strength and attenuate the effect of rough side borders (Yang, et al. (2019)). A numerical buckling analysis was conducted to verify that the sample length within the grip section was bellow the buckling limit under compression for the target load. A strain rate of $0.01\ \%/s$ was used for three elapsed cycles. As a loading, a tension-compression test with load amplitudes of $\pm$ 16 KN was applied over an external controlled program, which feeds the machine with a triangular ramp loading. According to the ISO-527-1 and ASTM-D3039 standards, the stiffness should be taken over a strain range of 0.2% (Iso E. 527-1. (2012), ASTM D3039. (2017)). The load level is chosen such that the deformation exceeds this range but still stay bellow load-levels where damage initiation could be introduced. The tensile-compression strain was measured at the four channels of the clip gauge extensometer.

10) Evaluation and comparison actually good. Good reasoning why the FS differs for both types of same trend. But how can the differences in the models be explained if everything has to be the same there (similar assumptions)? According to the type 1 statements, I would expect a similar trend to come out on the WS side for type 2. However, the "rough" model is better. Why?

Results of experiments in FS section should be the same for type 1 and 2?

Thanks for pointing that out. When it comes to experimental data, the flat section differs in results for type 1 and type 2 as the samples might deviate in fiber volume fraction or potential microcracks that can arise during the manufacturing process. As it comes to the difference in the model, that can be due to the slight difference in thickness for each type of wrinkle which was taken into account in the model. The difference between the surrogate and the high fidelity model for the flat section it can be due to slight differences in the mesh as the size of the mesh changes locally for the HFM due to the complex pattern of fold and resin epoxy.

The purpose of this analysis was to present that both models are capable of providing a good agreement with the experimental data. In a 2D model with assumptions of homogeneous fiber volume fraction, it is difficult to say that the rough model performs better than the high-fidelity one.

verified through correlations of FE simulations and the results from experimental tests. When it comes to experimental data, the stiffness at the flat section has a minor deviation comparing type 1 and type 2 configurations as the samples might deviate in fiber volume fraction or potential microcracks that can arise during the manufacturing process. When the deviation is observed in the numerical results, that is in principal due to a slight difference in thickness for each type of wrinkle which was taking into account in the model for both types of samples. Furthermore, the complexity of the geometrical features present in the HFM induce a different pattern of mesh where the local size of few elements are different from the SM which is simpler and therefore straightforward for a even sized mesh.

11) model prediction for flat section is better on tensile side opposite to compression side. And the other way round for wrinkle section. Can you explain these?

The explanation updated in the manuscript is as follows:

The stress vs per cent strain of coupon specimens shown in Figure 11 are obtained from averaging the extensometers results at the top and bottom of the wrinkle located in a gauge length of 50 mm around the center. The strain levels are also measured at the flat section, 40 mm away from the wrinkle center with an extensometer gauge length of 25mm. The results obtained
235 from the numerical models are extracted at the same position as the experiments. wrinkles are introducing an asymmetry in the experimental setup. The difference in stiffness in tensile and compression side will depend on the asymmetry if the test-geometry introduced by the winkle and thus on details on how the samples are clamped and alignment of the pistons. Therefore we are mainly focused on averaging the stiffness at the two sides what is done subsequently in the comparison.

12) Specify deviations

The error-bar show the actual stiffnesses values measured for the two samples of each of the two winkle types. Modifications below:

220 in the flat section. By comparing both configurations, the damping of type 1 wrinkle is 32% higher than type 2. Consequently, the higher the wrinkle angle, the higher the energy losses as a result of the shear loading of the resin in the wrinkle section.

Figure 10 shows the experimental results for stiffness in both types of specimens at the wrinkle section and flat section against the predictions pointed by the surrogate model and the high fidelity model along with respective average deviation. The error bars show the actual stiffness values measured for the two samples tested of each type of wrinkle. The numerical models are

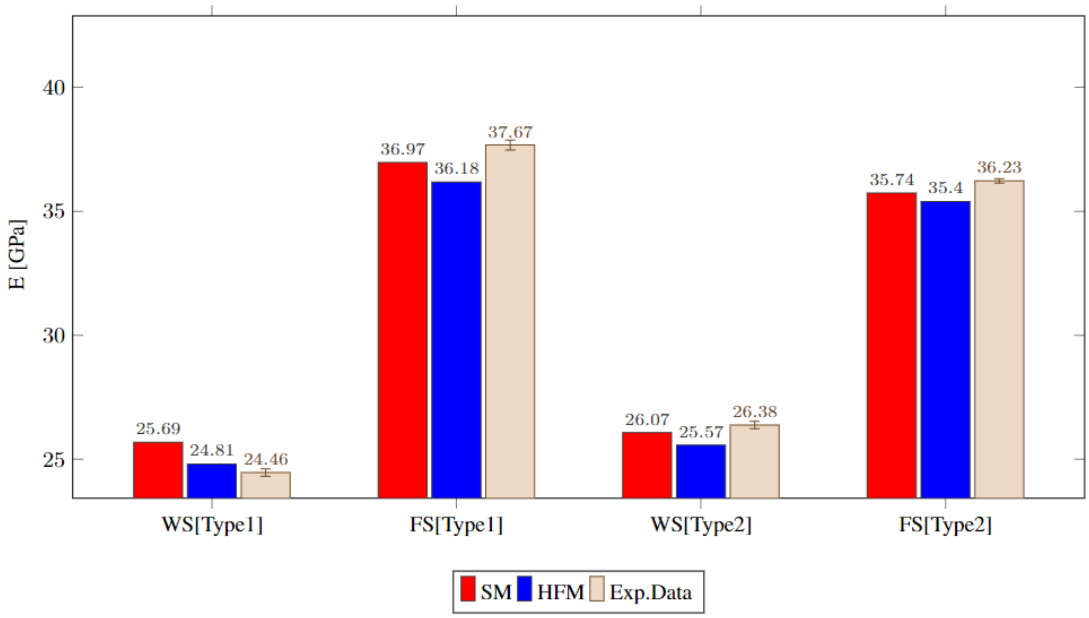

Figure 10. Stiffness results for wrinkles type 1 and type 2 around the wrinkle section (WS) and the flat section (FS) based on the numerical model predictions and experimental data.